



Earth system model simulations show different carbon cycle feedback strengths under glacial and interglacial conditions

Markus Adloff^{1,2,3}, Christian H. Reick¹, and Martin Claussen^{1,3}

¹Max Planck Institute for Meteorology, Bundesstraße 53, 20146 Hamburg, Germany

²now: School of Geographical Sciences, University of Bristol, University Road, BS8 1SS, United Kingdom

³Meteorological Institute, Centrum für Erdsystemforschung und Nachhaltigkeit (CEN), Universität Hamburg, Germany

Correspondence to: Markus Adloff (markus.adloff@bristol.ac.uk)

Abstract. In Earth system model simulations we find different carbon cycle sensitivities for recent and glacial climate. This result is obtained by comparing the transient response of the terrestrial carbon cycle to a fast and strong atmospheric CO₂ concentration increase (roughly 1000ppm) in C⁴MIP type simulations starting from climate conditions of the Last Glacial Maximum ("LGM") and from Pre-Industrial times ("PI"). The sensitivity β to CO₂ fertilization is larger in the LGM experiment during most of the simulation time: The fertilization effect leads to a terrestrial carbon gain in the LGM experiment almost twice as large as in the PI experiment. The larger fertilization effect in the LGM experiment is caused by the stronger initial CO₂ limitation of photosynthesis, implying a stronger potential for its release upon CO₂ concentration increase. In contrast, the sensitivity γ to climate change induced by the radiation effect of rising CO₂ is larger in the PI experiment for most of the simulation time. Yet, climate change is less pronounced in the PI experiment, resulting in only slightly higher terrestrial carbon losses than in the LGM experiment. The stronger climate sensitivity in the PI experiment results from the vastly more extratropical soil carbon under those interglacial conditions whose respiration is enhanced under climate change. Comparing the radiation and fertilization effect in a factor analysis, we find that they are almost additive, i.e. their synergy is small in the global sum of carbon changes. From this additivity, we find that the carbon cycle feedback strength is more negative in the LGM than in the PI simulations.

1 Introduction

During the last glacial maximum (21 000 yrs before present) vegetation was not only less widespread than today but also primary productivity was smaller (Prentice and Harrison, 2009). This is the consequence of the lower CO₂ concentrations during those times (about 200 ppm less than today), physically via the resulting lower temperatures (greenhouse effect), and biogeochemically via the reduced photosynthetic activity (CO₂ fertilization effect) (Prentice and Harrison, 2009). Today CO₂ concentrations are dramatically rising and are expected to rise at least by a similar magnitude (Flato et al., 2013). One might thus hope that an analysis of the past rise will help foreseeing what to expect.

Ideally, one could convert CO₂ concentration rise directly into climate and environmental changes. Accordingly, the climate community has put much effort in deriving a characteristic number for the global temperature rise induced per ppm CO₂ concentration rise, called "climate sensitivity". Values can be derived from paleo records and from numerical simulations



of past climates (see e.g. PALEOSENSE (2012); Royer (2016)). Despite these intense activities the resulting values are still subject to considerable uncertainty (PALEOSENSE, 2012; Royer, 2016). But even if one had an exact number for past climates, it would not be clear whether it could be applied to the future climate development. In fact, there is evidence for a state dependence of climate sensitivity (PALEOSENSE, 2012; Woillez et al., 2011; Claussen et al., 2013). In numerical simulations, this climate state dependence can be traced back to the different time scales of the forcing and feedback mechanisms (von der Heydt and Ashwin, 2016). There is also evidence that the strength of feedbacks in the climate system varies with boundary conditions (Caballero and Huber, 2013; Lunt et al., 2016)

One such feedback arises from the interaction between carbon cycle and climate. To characterize this feedback, Friedlingstein et al. (2003) introduced two carbon cycle sensitivities, both characterizing the change in stored carbon (terrestrial and/or ocean) but due to different drivers: due to a change in plant available atmospheric CO₂ (β sensitivity) and to a change in surface temperature (γ sensitivity). Values have been derived from numerous Earth system simulations, particularly within the international Coupled Climate Carbon Cycle Model Intercomparison Project (C⁴MIP)(see e.g. Friedlingstein et al. (2006); Ciais et al. (2013)). While these attempts concentrate on perturbations of the pre-industrial climate, attempts to study carbon sensitivities for perturbations of past climates are rare. They all relate reconstructions of atmospheric CO₂ concentrations to reconstructions of temperature (see Friedlingstein (2015) for a review). The resulting 'observed' sensitivity of atmospheric CO₂ concentration to temperature involves the combined effect of changing temperature and changing of plant available CO₂ and is thus neither measuring β nor γ as defined by Friedlingstein et al. (2003). An exception is the study by Frank et al. (2010), who considered temperature and CO₂ reconstructions for the last Millennium before the industrial revolution: Their estimate should be a good proxy for γ since during this time the changes in atmospheric CO₂ concentration have been only a few ppm. The γ sensitivity obtained in this way turns out to be compatible with the low end values found in the C⁴MIP studies.

Although the contribution of the fertilization and the radiation effect to the different vegetation distribution in modern and past times have been quantified (eg. Claussen et al. (2013), Woillez et al. (2011)), there seem to be no estimates of carbon cycle sensitivities from climate simulations of the past. This makes it difficult to estimate the role carbon cycle feedbacks play for the climate state dependence of the Earth system response to rising CO₂ concentrations. Yet this is a critical point when we want to learn from the past what future consequences of anthropogenic CO₂ emissions to expect. To work towards closing this gap, the present study compares the carbon cycle sensitivities of the Earth system at two different climatic conditions. In order to derive β and γ values for past and present we perform a set of C⁴MIP-type simulations starting from a climate state representing the last glacial maximum and compare it with a corresponding set of C⁴MIP-type simulations starting from a pre-industrial climate state (simulations 1pctCO2, esmFdbk1 and esmFixClim1 from C⁴MIP). In this way we obtain β and γ values for two drastically different climates within the same model setup to evaluate their climate state dependence and the causes for this dependence.

The paper is organized as follows: We begin with a detailed discussion of metrics for the analysis of carbon cycle feedbacks before applying them to the results of experiments described thereafter. Following that, we compare the different initial Earth system states in the two experiments, before analyzing the reaction to rising CO₂ concentration. We do this by calculating the



above mentioned sensitivities and the strength of the carbon cycle feedback. Finally we discuss the mechanisms underlying the differences in system behaviour.

2 Disentangling the two effects of rising CO₂ concentrations in simulations

There are two conceptionally different aspects of how rising CO₂ concentrations affect the terrestrial carbon cycle: A fertilization and a radiation effect. The fertilization effect leads to increased photosynthetic productivity due to more physiologically available CO₂ in the air but indirectly also to increased soil water availability because plants become more efficient in water use under increased CO₂ concentrations (see e.g. Chapin III et al. (2011)). The radiation effect is caused by the CO₂ acting as a greenhouse gas. The resulting climate change (temperature, precipitation, ...) alters the conditions for plant growth and decomposition of organic matter (litter, soils). While the strength of the fertilization effect is characterized by β , the radiation effect is characterized by γ .

To determine β and γ in Earth system simulations, we follow the C⁴MIP experimental design (Ciais et al., 2013, Box 6.4) for *concentration driven* simulations: Starting from a control simulation (“ctrl”) performed at constant CO₂ concentration, two transient simulations forced by rising CO₂ concentrations are performed. In the first of those transient simulations (“fert”) only the fertilization effect is active, which means that the rising CO₂ concentration is “seen” only by the photosynthesis code of the model, while the radiation code constantly “sees” the CO₂ value of the control simulation. Conversely, in the second transient simulation (“rad”) only the radiation effect is active, i.e. only the radiation code “sees” the rising CO₂ concentrations but not the photosynthesis model. In addition we perform a third fully coupled transient simulation (“full”), where both effects are simultaneously active. One reason for this additional simulation is to supplement our sensitivity analysis by a factor analysis following Stein and Alpert (1993) to quantify also the synergies between the two effects.

Our analysis focusses on changes in land carbon, denoted as C in the following. For this variable the factor analysis proceeds as follows. The pure effects of fertilization and radiation are contained in the differences

$$\begin{aligned}\Delta C_{fert}(t) &:= C_{fert}(t) - C_{ctrl} \\ \Delta C_{rad}(t) &:= C_{rad}(t) - C_{ctrl}\end{aligned}\tag{1}$$

where the indices at the right hand side C -values refer to the simulations from which the values were obtained, while the indices to the ΔC -values refer to the effect considered. The time dependence t appears only for the values from the transient simulations, but not from the control simulations where the amount of terrestrial carbon is equilibrated in a spin up simulation. In addition the synergy is that part of the land carbon storage difference between the “full” and “ctrl” simulation that cannot be explained by an addition of the individual fertilization and radiation effects, i.e.

$$\Delta C_{syn}(t) := (C_{full}(t) - C_{ctrl}) - (\Delta C_{fert}(t) + \Delta C_{rad}(t)).\tag{2}$$



To obtain the β and γ sensitivities one must consider also differences in land temperature and atmospheric CO₂ concentration that develop in the transient simulations. Of particular interest are

$$\begin{aligned}\Delta T_{rad}(t) &:= T_{rad}(t) - T_{ctrl} \\ \Delta c(t) &:= c(t) - c_{ctrl}.\end{aligned}\quad (3)$$

The concentration of atmospheric CO₂ is denoted here by a small “ c ” and measured in ppm CO₂. Since $c(t)$ is the same for the transient simulations performed here, the index referring to the type of experiment has been omitted. With these definitions the two sensitivities are defined as

$$\begin{aligned}\beta(t) &:= \frac{\Delta C_{fert}(t)}{\Delta c(t)} \\ \gamma(t) &:= \frac{\Delta C_{rad}(t)}{\Delta T_{rad}(t)}.\end{aligned}\quad (4)$$

Finally, this analysis framework allows to quantify the strength of the carbon climate feedback. For this, in addition to γ and β , we need to know the response of temperature to increasing CO₂ concentrations, expressed by the climate sensitivity α :

$$\alpha(t) := \frac{\Delta T_{rad}(t)}{\Delta c(t)}\quad (5)$$

In the considered concentration driven C⁴MIP experiment set up, the carbon flux from the atmosphere to land carbon pools does not feed back on the atmospheric CO₂ concentration because the latter is prescribed. Still, the feedback strength f and the carbon gain g of the land carbon pools characterizing the carbon cycle feedback to rising CO₂ concentration can be diagnosed (Gregory et al., 2009; Arora et al., 2013). Supposing that the radiation and the fertilization effect as characterized by the sensitivities β and γ add up linearly, the cumulated carbon influx to the atmosphere until time t consistent with the atmospheric CO₂ is

$$I_{tot}(t) = m\Delta c(t) = I_{ext}(t) - \alpha(t)\gamma(t)\Delta c(t) - \beta(t)\Delta c(t),\quad (6)$$

where I_{ext} is the cumulated carbon flux from external sources of emissions and $m = 2.12 \cdot 10^6$ Pg is the conversion factor from atmospheric CO₂ concentration to atmospheric CO₂ mass (Flato et al. (2013), page 471). In this diagnostic carbon balance the terms for the feedback contributions from the radiation and fertilization effects enter with a minus sign because by definition positivity of α and β mean land carbon uptake and thus atmospheric carbon loss. Contributions from the ocean response to changes in CO₂ could be omitted in (6) since in the experiments considered here atmospheric CO₂ is prescribed. Following Friedlingstein et al. (2003) the feedback factor $f(t)$ and gain $g(t)$ can now be defined as

$$I_{tot}(t) =: f(t)I_{ext}(t) =: \frac{1}{1 - g(t)}I_{ext}(t).\quad (7)$$

By solving for $\Delta c(t)$ one obtains from (6) and the definitions (7)

$$\begin{aligned}f(t) &= \frac{m}{m + \alpha(t)\gamma(t) + \beta(t)} \\ g(t) &= -\frac{\alpha(t)\gamma(t) + \beta(t)}{m}\end{aligned}\quad (8)$$

Note that in this framework also α , β and γ are time dependent – a point that will be further discussed below.



3 Experiment set up

This paper focusses on the difference of the carbon cycle response to rising CO₂ concentrations in glacial and pre-industrial times. Accordingly, for each case we need a set of four simulations (ctrl, rad, fert, full) to calculate sensitivities and feedback strength. In the following, we will use the term 'experiment' to refer to one of the two cases LGM or PI. 'Simulation' will refer to one of the four model runs ctrl, rad, fert or full. For the LGM case the simulations start with Last Glacial Maximum (LGM) conditions (185 ppm) and those of the other experiment start with Pre-Industrial (PI) conditions (285 ppm). We did not run the simulations for the PI experiment anew but chose to use the published CMIP5 simulations piControl, esmFdbk1, esmFixClim1 and 1pctCo2 and to set up the LGM experiment accordingly, using the same model version. The LGM simulations are initialized with restart files from an existing last glacial maximum spin-up experiment (1800 simulation years long) followed by 200 years for the adaptation of dynamic vegetation (Jungclaus et al., 2014). The PI simulations are initialized with a spin-up experiment simulating climate conditions of the early 19th century over more than 3000 years (Giorgetta et al., 2012). For the transient simulations fert, rad and full, the same absolute increase in atmospheric CO₂ concentration is simulated in both experiments over a period of 150 years (see Fig. 1) with the full (for simulation "full") and partially coupled (for simulations "fert" and "rad") Earth system.

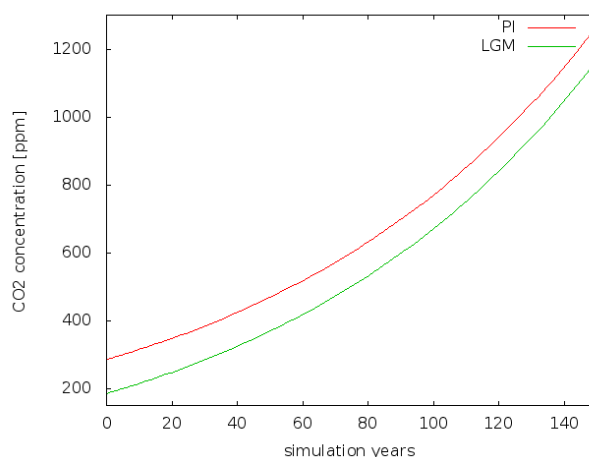


Figure 1. CO₂ scenarios ($\Delta c(t)$ in previous equations) as prescribed for the LGM and PI experiments: Starting from 185ppm ("Last Glacial Maximum", green line) and starting from 285ppm ("Pre-Industrial", red line).

The experiments are conducted with the Earth-System Model of the Max Planck Institute (MPI-ESM, compare Giorgetta (2013)). The MPI-ESM consists of the atmosphere component ECHAM6 and the ocean component MPIOM. The terrestrial processes including carbon cycle and dynamic biogeography are calculated in the land surface model JSBACH. Because atmospheric CO₂ concentrations are prescribed in our experiments, the oceanic and terrestrial carbon cycles are decoupled so that changes in the ocean carbon cycle are irrelevant here; nevertheless the physical ocean remains an important component of the climate dynamics. JSBACH comprises the DYNVEG model for simulation of natural land cover changes (Reick et al.,



2013) and the BETHY model (Knorr, 2000) for representation of the fast processes of the biosphere, building on primary production rates that are simulated following the Farquhar model (Farquhar et al., 1980) for C3 and Collatz model (Collatz et al., 1992) for C4 photosynthesis. Vegetation is represented by eight plant functional types that differ in phenology and physiology and interact dynamically (see Brovkin et al. (2013) for an evaluation of the present implementation of dynamic
5 biogeography). Anthropogenic land cover change is not included in the experiments conducted here. Terrestrial carbon pool dynamics are calculated with CBALANCE (Reick et al., 2010), simulating temperature- and water scarcity dependent carbon fluxes between seven carbon pools with different overturning periods.

4 Differences in the initial Earth system states

Globally, mean near surface temperatures are 4.5 K colder in the LGM state (LGM control simulation) than in the PI state (PI
10 control simulation) but locally, temperatures differ by 20 K and more (see Fig. 2). Soil water levels are mostly higher in the LGM state, especially in the tropics and subtropics. Inland glaciers extend throughout most of North America and northern Europe and the sea level is considerably lower, leading to more landmasses, especially in the Bering Strait and the Indonesian archipel. On global scale, less area is covered by vegetation in the LGM state and dense vegetation is restricted to the tropical zone (compare Fig. 3). In the PI state, vegetation reaches far more into the extratropics and the mid latitudes are more densely
15 covered by vegetation.

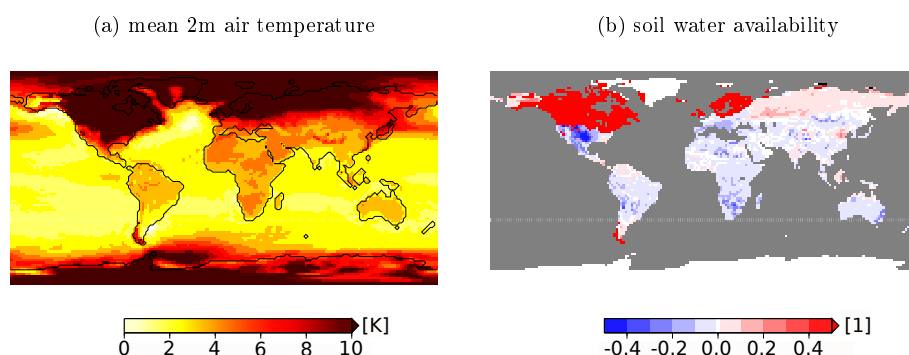


Figure 2. Differences between the initial climates of the LGM and PI experiments: a) Difference between global mean near surface temperatures and b) difference between soil water availabilities. The values in the LGM initial state are subtracted from the values in the PI initial state. Land areas that are covered by ice in the LGM but not PI initial state show values > 0.4 in the water availability differences.

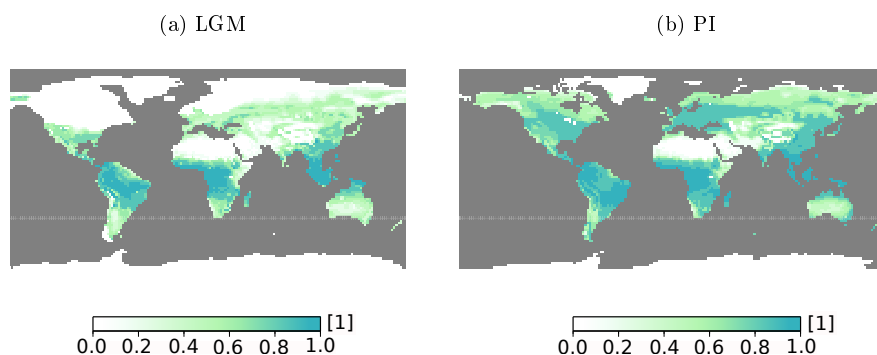


Figure 3. Potential vegetation cover in the initial states of the experiments. The degree of coverage is given in vegetation covered fractions per grid cell.

5 Reaction of the Earth system to rising CO₂ concentration under different boundary conditions

The climate system reacts differently to rising CO₂ concentrations for LGM and PI conditions. Fig. 4 shows changes in global mean near surface temperature and soil water availability in both experiments. Due to rising CO₂ concentrations, the global mean near surface temperature rises and soil water availability decreases in the global integral. Both changes are larger in the LGM experiment. The temperature increases mainly due to the radiation effect of rising CO₂ concentrations; CO₂ fertilization and synergistic effects do not considerably affect global mean near surface temperature (not shown). The globally averaged soil water availability, on the contrary, rises due to increased water use efficiency in connection with the fertilization effect and decreases due to higher evapotranspiration losses under the higher temperatures as a consequence of the radiation effect. In the fully coupled run, the decrease due to climate change dominates.

Figure 5 shows the change of terrestrial carbon pool size due to the prescribed CO₂ concentration increase scenario. Overall, terrestrial carbon pool size increases in response to the rising CO₂ concentration in both experiments, which is due to the fertilization effect. The fertilization is stronger in the LGM than in the PI experiment. The radiation effect is negative and of similar strength in the two experiments. Synergies of both effects are small in the global integral. The last point is especially important as it shows that linear additivity of the radiation and fertilization effect can be assumed on the global scale to derive the feedback strength and gain.

From Fig. 5 it becomes clear that the same absolute increase in atmospheric CO₂ concentration triggers different reactions of the terrestrial carbon pool in the differently initiated simulations. This is reflected in the corresponding sensitivities as shown in Fig. 6. There, the sensitivity values for the LGM and PI experiments are shown as a function of simulation time. In the following, the sensitivities to the radiation and fertilization effects will be studied one after the other, before discussing the combined feedback strength.

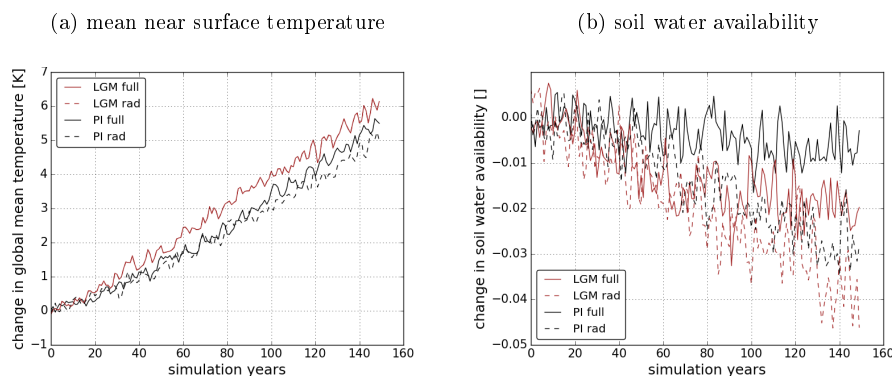


Figure 4. Climatic changes in the fully coupled run (continuous lines) and radiatively coupled run (dashed lines) due to rising CO₂ concentrations in the LGM experiment (red) and PI experiment (black). a) shows the globally averaged change in near surface temperature and b) in soil water availability.

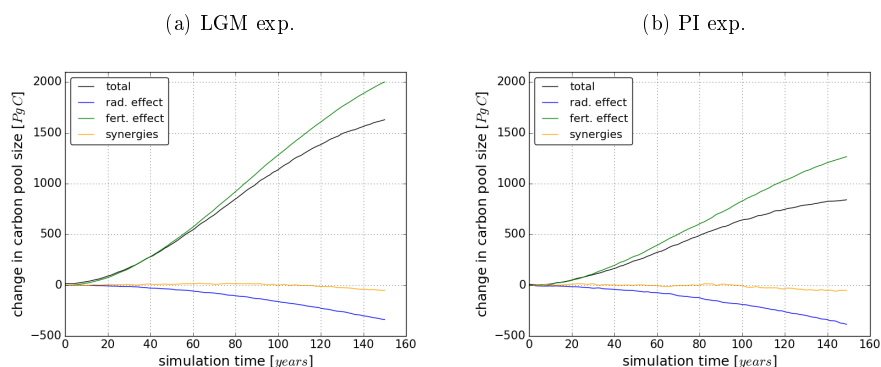


Figure 5. Change in terrestrial carbon storage [PgC] in the fully coupled simulation (black curve) and split into factors (coloured curves) as deviation from the control simulation (a) in the LGM experiment and (b) in the PI experiment.

5.1 The fertilization effect

In both experiments, β increases in the beginning of the experiment. But already for simulation times larger than 30 to 40 years, the increase slows down. Arora et al. (2013) attribute this behaviour to the difference in response time of primary production and biomass decomposition. While productivity increases almost instantaneously with increasing physiologically available CO₂, biomass decomposition remains initially unchanged and only increases when, in consequence of the higher productivity, after a temporal delay more biomass is transferred to litter and soil carbon pools. Additionally - and this is found to be the main effect in the present study - the fertilization effect becomes less effective at high productivity levels because carbon density of living vegetation is reaching upper limits. In fact, the amount of carbon allocatable to biomass carbon pools is restrained in JSBACH to account for a down regulation of carbon allocation when structural limits are hit. During the entire simulation

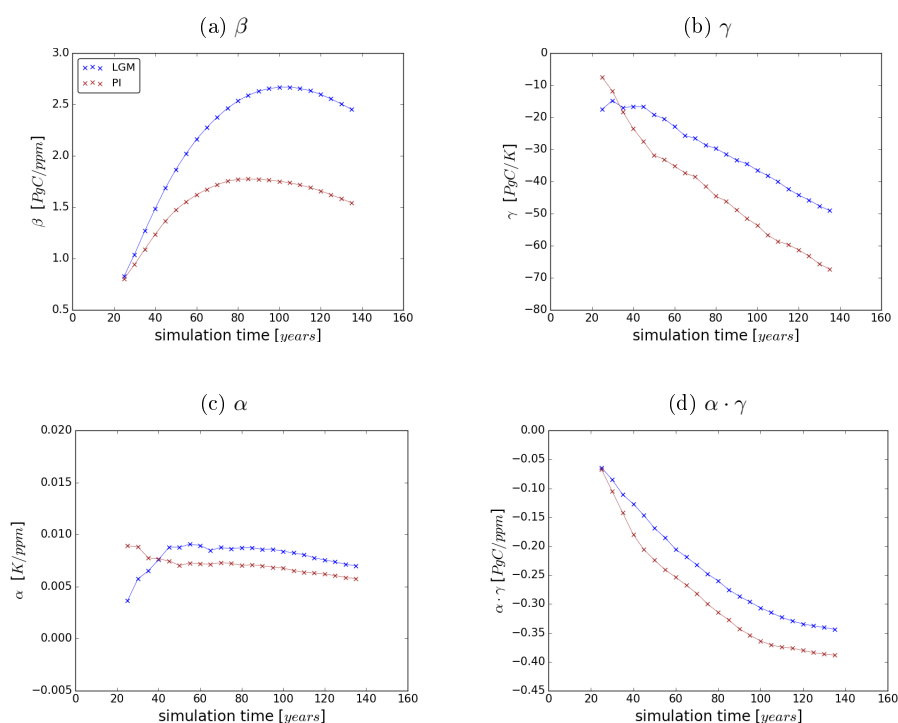


Figure 6. Sensitivities β and γ to the fertilization and radiation effect (respectively) of rising CO_2 concentrations and climate sensitivity α in the LGM (blue) and the PI experiment (red).

time, β is larger in the LGM experiment than in the PI experiment. This is caused by the lower initial CO_2 concentration. In both initial states, photosynthesis is carboxylation rate limited. In other words, the initial atmospheric CO_2 concentrations are too low as to allow for maximum photosynthetic exploitation of the insolation. This initial CO_2 limitation is lifted by the increasing CO_2 concentration and leads to increasing primary productivity that allows for vegetation cover extension and increasing terrestrial carbon pool sizes. As long as the CO_2 availability stays to be the main limitation for productivity, the fertilization effect of rising CO_2 concentration leads to large increases in productivity. In our experiments, the simulated CO_2 concentration rise is however large enough to reach a point where insolation becomes more limiting to productivity than the CO_2 availability. The transition is clearly visible in Fig. 7, where the modeled dependence of primary production rate on CO_2 concentration is shown for the eight vegetation types present in our simulations.

From that transition point on, the effectivity of CO_2 fertilization is reduced. The prescribed CO_2 forcing is such that the difference in CO_2 concentration between the two experiments remains the same throughout the simulation time. However, because the CO_2 concentration is raised beyond the point of effectivity change, the stronger initial CO_2 limitation of the LGM experiment is more important for the fertilization effect than the higher final concentration in the PI experiment. Therefore,

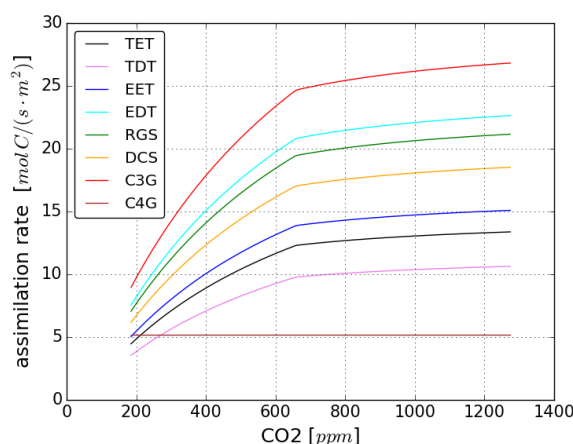


Figure 7. Dependence of gross assimilation per m^2 leaf on air CO_2 concentration according to the implemented photosynthesis model (Farquhar et al., 1980) for C3 plant physiology at 20°C leaf temperature. Abbreviations stand for individual vegetation types: TET for tropical evergreen trees, TDT for tropical deciduous trees, EET for extratropical evergreen trees, EDT for extratropical deciduous trees, RGS for raingreen shrubs, DCS for deciduous shrubs, C3G for C3 grasses and C4G for C4 grasses.

although the final CO_2 concentration is larger in the PI experiment, the fertilization effect is larger in the LGM experiment. The stronger CO_2 fertilization in the LGM experiment is mostly due to the strong reaction of tropical vegetation. In the extratropics, the fertilization effect is stronger in the PI experiment but still does not reach the tropical production rate increases of the LGM experiment.

5

5.2 The radiation effect

γ grows increasingly negative in both experiments (see Fig. 6). It is increasingly larger in absolute value in the PI experiment than in the LGM experiment. Although γ differs clearly in the two experiments, the overall terrestrial carbon pool changes in the radiatively coupled simulations are almost similar (compare Fig. 5). The reason for this is that also the climate sensitivity α varies between the two experiments. α is larger in the LGM experiment over the entire simulation time. The higher climate sensitivity and the lower carbon cycle sensitivity γ partially compensate differences between the PI and LGM cases as is seen from Fig. 6 (d) where the product $\alpha\gamma$ has been plotted; it is this combination of sensitivities that describes the total radiative effect on carbon losses (compare equation (6)). Thereby the radiation effect on land carbon storage differs much less between the LGM and PI case than the fertilization effect discussed above.

15 To understand the processes behind the different γ sensitivity in the two experiments, it is useful to analyze first how climate change induces carbon losses differently in the tropics and extratropics. Table 1 lists the change per degree temperature change in soil respiration ΔR_s relative to the one in net primary productivity ΔNPP separately for tropics and extratropics



in the two 'rad' simulations. In both simulations this ratio is smaller than one in the tropics (more land carbon input change than output change) but larger than one in the extratropics (more land carbon output change than input change), indicating a very different functioning of the carbon cycle under climate change in these two regions. Considering first the tropics, net primary productivity and soil respiration decrease (see table), indicating that living conditions deteriorate here. This has two reasons: First, its getting drier so that plant productivity and also soil decomposition are reduced. Second, the already hot tropical climate is getting even hotter during the simulations so that physiological limits are hit more frequently thereby deteriorating plant productivity by damaging the photosynthetic apparatus (implemented as 'heat inhibition' in MPI-ESM). But the reduction in NPP is much larger than the reduction in soil respiration. Hence in the tropics land carbon losses are mostly driven by reduced plant productivity. In the extratropics the situation is different: rising values of NPP and R_s (see table) are well understandable because under the warming climate physiological processes speed up there. But since ultimately R_s is fed from NPP, the considerably larger increase in R_s cannot be a result of the enhanced carbon input. Instead, it results from the enhanced decomposition of soil carbon that had accumulated in those vast cold boreal areas already in the control simulation. Hence in the extratropics land carbon losses are mostly driven by enhanced soil respiration of 'old' carbon.

Having identified the major drivers for carbon losses in the tropics and extratropics, one can now understand why the temperature sensitivity γ is larger in the PI than in the LGM simulation. In the tropics plant productivity reduction is the major driver, and productivity reacts more sensitive in the PI than the LGM simulation (see table 1) because tropical living conditions deteriorate from already initially drier and hotter conditions. And in the extratropics enhancement of soil respiration was found to be the major driver, and soil respiration reacts more sensitive in the PI than in the LGM simulation (see table 1) because of the vegetation extending much farther north under the warmer conditions and in absence of ice sheets going along with vastly more extratropical 'old' soil carbon getting respired. Hence both in the tropics and in the extratropics the land carbon cycle is more sensitive to climate change in the PI case. Furthermore, table 1 shows that the larger sensitivity of the extratropics dominates the one in the tropics.

Table 1. Temperature sensitivity of net primary productivity NPP and soil respiration R_s due to the radiative effect. Sensitivities are computed from changes ΔNPP and ΔR_s per temperature change ΔT . Additionally, the relative change of soil respiration (soil respiration change divided by NPP change) is given in the last row. The change of the carbon fluxes over the entire simulation time (end values minus start values), integrated over the Earth's surface and all vegetation types is divided by the regional temperature change over the same period. 'Tropics' refers here to the latitudinal belt between 30° South and 30° North and 'extratropics' to the remaining part of the globe. Here, ΔNPP and ΔR_s are considered positive for plant carbon uptake and soil carbon loss, respectively.

sensitivity [PgC/K]	tropics		extratropics	
	LGM	PI	LGM	PI
$\Delta NPP/\Delta T$	-134.6	-151.2	10.8	28.6
$\Delta R_s/\Delta T$	-55.9	-49.7	17.1	48.2
$\Delta R_s/\Delta NPP$	0.42	0.33	1.59	1.69



5.3 Feedback strength and atmospheric carbon gain

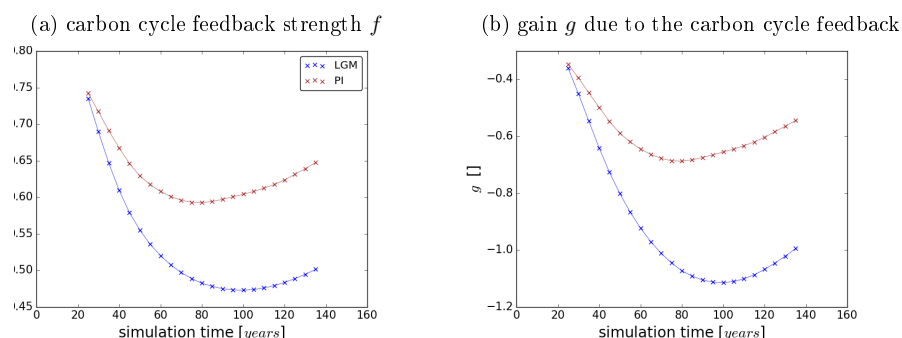


Figure 8. Feedback strength f and atmospheric carbon gain factor g for the overall feedback of the carbon cycle to the imposed CO_2 forcing in the LGM and the PI experiment.

Due to the the radiation and the fertilization effect, the reacting terrestrial carbon pool produces a feedback to the initial CO_2 forcing. The strength of this terrestrial carbon cycle feedback is lower than 1 (see figure 8 (a)), showing that the total carbon cycle feedback to rising CO_2 concentrations dampens the effect of the forcing so that less carbon is left in the atmosphere than injected by the forcing. Accordingly, the feedback is negative, as also visible from the gain factor (figure 8 (b)). This effect is stronger in the LGM experiment, especially towards the end of the simulations, due to the larger value of β . The stronger negative carbon cycle feedback in the LGM experiment would, in case of a prescribed amount of carbon input, lead to a reduced increase in atmospheric CO_2 concentration compared to the PI experiment. From the more negative LGM gain factor it is also understandable that despite identical concentration scenarios in the two experiments, the absolute mass of carbon introduced to the system by the end of the simulation is larger in the LGM experiment. The recovery of f and g towards the end of the simulation is mostly a consequence of the recovery of β (compare figure 6 (a)) for the reasons explained in section 5.1.

6 Discussion and Conclusion

Results from the different phases of C^4MIP demonstrate that β and γ vary largely with the employed Earth system model (see Arora et al. (2013) and the third data column in table 2). The γ values of the LGM and the PI experiment obtained in the present study lie inside the inter-model range for the preindustrial γ whereas the glacial β is larger than any preindustrial β from the inter-model comparison. It is important to mention that there is a difference in the CMIP values for the MPI-ESM and those calculated from the PI experiment in the present study. The latter consider only natural vegetation types to improve the comparability of the anthropogenically unperturbed LGM and the anthropogenically perturbed PI states of the biosphere. In contrast, anthropogenic bioms are included in the calculations of the CMIP values, which lead to larger absolute values of β and γ than with natural vegetation only. Additionally, a different time averaging is applied.



Table 2. β and γ sensitivities at the end of the LGM and PI experiments and their inter-model range according to Arora et al. (2013) for the PI experiment, considering only models without nitrogen cycle.

sensitivity value	LGM exp.	PI exp.	Arora et al. (2013)
β [PgC/ppm]	2.07	1.33	0.74 – 1.46
γ [PgC/K]	-44.0	-74.4	-30.1 – -88.6

While the difference in sensitivities between the LGM and the PI experiments can be traced back to different initial conditions in these experiments, there is still a strong dependence on the forcing pathway and its absolute amplitude. For example, the difference in β largely depends on whether the forcing is strong enough to produce a switch from carboxylation rate limited to electron transport limited assimilation. Additionally bioclimatic limits of vegetation, maximum productivity rates, the choice of the wilting point and maximum carbon pool sizes introduce transition points to the system that shape the behaviour of terrestrial carbon pools, which, in consequence, will show different reactions to forcings of different amplitudes. From the employed set up and sensitivity measures, it is therefore not possible to derive and compare equilibrium sensitivities which should be independent of the forcing scenario and could ideally be understood as a system property to characterise an Earth system state as such. Additionally, the absolute sensitivity and feedback values – including those found in the present study – must be considered with care since not yet all adaptational strategies of vegetation to changing climate and CO_2 concentration are known (e.g. Christmas et al. (2015)) and implemented in numerical models. But even if one is sceptical about the realism of the numbers obtained for the LGM and PI sensitivities, the present study has demonstrated that they can be used to understand why the Earth system may react differently to rising CO_2 concentrations under LGM and PI conditions. In the two experiments, the terrestrial biosphere and carbon pools react differently to the same absolute increase in atmospheric CO_2 concentration. It can therefore be concluded that there is a climate state dependence in the transient reaction of the terrestrial carbon cycle to increasing CO_2 concentrations in these experiments. More precisely, for LGM conditions, the carbon flux balance is more sensitive to the fertilization effect than in PI conditions. This is due to a more severe CO_2 limitation of primary productivity in the LGM initial state that provides more potential for relaxation. The sensitivity to the radiation effect, in contrast, is larger under PI conditions which is caused by higher initial temperatures and larger extratropical terrestrial carbon pools in the PI initial state.

7 Code availability

The model code is publicly available after registration at www.mpimet.mpg.de/en/science/models/license.



8 Data availability

Simulation data are available on request from the authors.

Author contributions. The study was lead by M. A. who also performed the simulations and data analysis. All authors contributed to the design of the study and the manuscript.

5 *Competing interests.* None.

Disclaimer. None.

Acknowledgements. We would like to thank Irina Fast and the DKRZ team for their technical support and Gitta Lasslop for her careful comments on the final version of our draft.



References

- Arora, V. K., Boer, G. J., Friedlingstein, P., Eby, M., Jones, C. D., Christian, J. R., Bonan, G., Bopp, L., Brovkin, V., Cadule, P., Hajima, T., Ilyina, T., Lindsay, K., Tjiputra, J. F., and Wu, T.: Carbon-Concentration and Carbon-Climate Feedbacks in CMIP5 Earth System Models, *Journal of Climate*, 26, 5289–5314, 2013.
- 5 Brovkin, V., Boysen, L., Raddatz, T., Gayler, V., Loew, A., and Claussen, M.: Evaluation of vegetation cover and land-surface albedo in MPI-ESM CMIP5 simulations, *Journal of Advances in Modeling Earth Systems*, 5, 48–57, doi:10.1029/2012MS000169, 2013.
- Caballero, R. and Huber, M.: State-dependent climate sensitivity in past warm climates and its implications for future climate projections, *Proceedings of the National Academy of Sciences of the United States of America*, 110, 14 162–14 267, 2013.
- Chapin III, F., Matson, P. A., and Vitousek, P.: *Principles of Terrestrial Ecosystem Ecology*, Springer, New York, 2nd edn., 2011.
- 10 Christmas, M. J., Breed, M. F., and Lowe, A. J.: Constraints to and conservation implications for climate change adaptation in plants, *Conservation Genetics*, pp. 305–320, 2015.
- Ciais, P., Sabine, C., Bala, G., Bopp, L., Brovkin, V., Canadell, J., Chhabra, A., an J. Galloway, R. D., Heimann, M., Jones, C., Quéré, C. L., Myneni, R. B., Piao, S., and Thornton, P.: Carbon and Other Biogeochemical Cycles, in: *Climate Change 2013: The Physical Science Basis. Contribution of Working Group I to the Fifth Assessment Report of the Intergovernmental Panel on Climate Change*, edited by
- 15 Stocker, T., Qin, D., Plattner, G.-K., Tignor, M., Allen, S., Boschung, J., Nauels, A., Xia, Y., Bex, V., and Midgley, P., pp. 465–570, Cambridge University Press, Cambridge, UK, and New York, NY, USA, 2013.
- Claussen, M., Selent, K., Brovkin, V., Raddatz, T., and Gayler, V.: Impact of CO₂ and climate on Last Glacial maximum vegetation – a factor separation, *Biogeosciences*, 10, 3593–3604, 2013.
- Collatz, G. J., Ribas-Carbo, M., and Berry, J. A.: Coupled photosynthesis-stomatal conductance model for leaves of C₄ plants, *Australian*
- 20 *Journal for Plant Physiology*, 19, 519–538, 1992.
- Farquhar, G. D., Caemmerer, S., and Berry, J.: A biochemical model of photosynthesis in leaves of C₃ species, *Planta*, 149, 78–90, 1980.
- Flato, G., Marotzke, J., Abiodun, B., Braconnot, P., Chou, S., Collins, W., Cox, P., Driouech, F., Emori, S., Eyring, V., Forest, C., Gleckler, P., Guilyardi, E., Jakob, C., Kattsov, V., Reason, C., and Rummukainen, M.: Evaluation of Climate Models, in: *Climate Change 2013: The Physical Science Basis. Contribution of Working Group I to the Fifth Assessment Report of the Intergovernmental Panel on Climate*
- 25 *Change*, edited by Stocker, T., Qin, D., Plattner, G.-K., Tignor, M., Allen, S., Boschung, J., Nauels, A., Xia, Y., Bex, V., and Midgley, P., pp. 741–866, Cambridge University Press, Cambridge, UK, and New York, NY, USA, 2013.
- Frank, D. C., Esper, J., Raible, C. C., Buntgen, U., Trouet, V., Stocker, B., and Fortunat, J.: Ensemble reconstruction constraints on the global carbon cycle sensitivity to climate, *Nature*, 463, 527–530, 2010.
- Friedlingstein, P.: Carbon cycle feedbacks and future climate change, *Phil. Trans. R. Soc. A*, 373, 2014 042, 2015.
- 30 Friedlingstein, P., Dufresne, J.-L., Cox, P. M., and Rayner, P.: How positive is the feedback between climate change and the carbon cycle?, *Tellus*, pp. 692–700, 2003.
- Friedlingstein, P., Cox, P., Betts, R., Bopp, L., von Bloh, W., Brovkin, V., Cadule, P., Doney, S., Eby, M., Fung, I., Bala, G., John, J., Jones, C. D., Joos, F., Kato, T., Kawamiya, M., Knorr, W., Lindsay, K., Metthews, H. D., Raddatz, T., Rayner, P., Reick, C., Roeckner, E., Schnitzler, K.-G., Schnur, R., Strassmann, K., Weaver, A. J., Yoshikawa, C., and Zeng, N.: Climate-Carbon Cycle Feedback Analysis: Results from the C⁴MIP Model Intercomparison, *Journal of Climate*, pp. 3337–3353, 2006.
- Giorgetta, M., Jungclaus, J., Reick, C. H., Legutke, S., Brovkin, V., Crueger, T., Esch, M., Fieg, K., Glushak, K., Gayler, V., Haak, H., Hollweg, H.-D., Kinne, S., Kornbluh, L., Matei, D., Mauritsen, T., Mikolajewicz, U., Müller, W., Notz, D., Raddatz, T., Rast, S., Roeckner,



- E., Salzmann, M., Schmidt, H., Schnur, R., Segschneider, J., Six, K., Stockhause, M., Wegner, J., Widmann, H., Wieners, K.-H., Claussen, M., Marotzke, J., and Stevens, B.: CMIP5 simulations of the Max Planck Institute for Meteorology (MPI-M) based on the MPI-ESM-LR model: The piControl experiment, served by ESGF, World Data Center for Climate, doi:10.1594/WDCC/CMIP5.MXELpc, 2012.
- Giorgetta, M. A.: Climate and carbon cycle changes from 1850 to 2100 in MPI-ESM simulations for the Coupled Model Intercomparison Project phase 5, *Journal of Advances in Modeling Earth Systems*, 5, 572–597, 2013.
- 5 Gregory, J. M., Jones, C. C., Cadule, P., and Friedlingstein, P.: Quantifying Carbon Cycle Feedbacks, *Journal of Climate*, 22, 5232–5250, 2009.
- Hajima, T., Tachiiri, K., Ito, A., and Kawamiya, M.: Uncertainty of Concentration–Terrestrial Carbon Feedback in Earth System Models, *Journal of Climate*, 27, 3425–3445, doi:10.1175/JCLI-D-13-00177.1, 2014.
- 10 Jungclaus, J., Giorgetta, M., Reick, C. H., Legutke, S., Brovkin, V., Crueger, T., Esch, M., Fieg, K., Fischer, N., Glushak, K., Gayler, V., Haak, H., Hollweg, H.-D., Kinne, S., Kornbluh, L., Matei, D., Mauritsen, T., Mikolajewicz, U., Müller, W., Notz, D., Pohlmann, T., Raddatz, T., Rast, S., Roeckner, E., Salzmann, M., Schmidt, H., Schnur, R., Segschneider, J., Six, K., Stockhaus, M., Wegner, J., Widmann, H., Wieners, K.-H., Claussen, M., Marotzke, J., and Stevens, B.: cmip5 output2 MPI-M MPI-ESM-P lgm, served by ESGF, World Data Center for Climate. CERA-DB "MXEPIg2", 2014.
- 15 Knorr, W.: Annual and interannual CO₂ exchanges of the terrestrial biosphere: Process-based simulations and uncertainties, *Global Ecology and Biogeography*, 9, 225–252, 2000.
- Lunt, D., Farnsworth, A., Lopston, C., Foster, G. L., Markwick, P., O'Brien, C. L., Pancost, R. D., Robinson, S. A., and Wrobel, N.: Paleogeographic controls on climate and proxy interpretation, *Clim. Past*, 12, 1181–1198, 2016.
- PALEOSENSE: Making sense of palaeoclimate sensitivity, *Nature*, 491, 683–691, 2012.
- 20 Peng, J., Dan, L., and Huang, M.: Sensitivity of Global and Regional Terrestrial Carbon Storage to the Direct CO₂ Effect and Climate Change Based on the CMIP5 Model Intercomparison, *PLOS One*, 9, e95 282, doi:10.1371/journal.pone.0095282, 2014.
- Prentice, I. and Harrison, S.: Ecosystem effects of CO₂ concentration: evidence from past climates, *Climate of the Past*, 5, 297–307, 2009.
- Reick, C., Raddatz, T., Pongratz, J., and Claussen, M.: Contribution of anthropogenic land cover change emissions to pre-industrial atmospheric CO₂, *Tellus B*, 62, 329–336, 2010.
- 25 Reick, C. H., Raddatz, T., Brovkin, V., and Gayler, V.: The representation of natural and anthropogenic land cover change in MPI-ESM, *Journal of Geophysical Research*, 5, 1–24, 2013.
- Royer, D. L.: Climate Sensitivity in the Geologic Past." 0 (2015)., *Annual Review of Earth and Planetary Sciences*, 44, 277–293, 2016.
- Stein, U. and Alpert, P.: Factor Separation in Numerical Simulations, *Journal of the Atmospheric Sciences*, 50, 2107–2115, 1993.
- von der Heydt, A. S. and Ashwin, P.: State-dependence of climate sensitivity: attractor constraints and paleoclimate regimes, arXiv preprint, 30 2016.
- Willez, M.-N., Kageyama, M., Krinner, G., de Noblet-Ducoudré, N., Viovy, N., and Mancip, M.: Impact of CO₂ and climate on the Last Glacial Maximum vegetation: results from the ORCHIDEE/IPSL models, *Clim. Past*, 7, 557–577, 2011.